PHILOSOPHICAL TRANSACTIONS OF THE ROYAL SOCIETY B

Phil. Trans. R. Soc. B (2012) **367**, 1140–1154
doi:10.1098/rstb.2011.0205

Review

The blueprint of the type-3 injectisome

Agata Kosarewicz[1,2], Lisa Königsmaier[1,2] and Thomas C. Marlovits[1,2,*]

[1]*Research Institute of Molecular Pathology, Dr. Bohr Gasse 7, A-1030 Vienna, Austria*
[2]*Institute of Molecular Biotechnology, Austrian Academy of Sciences, Dr. Bohr Gasse 5, A-1030 Vienna, Austria*

Type-3 secretion systems are sophisticated syringe-like nanomachines present in many animal and plant Gram-negative pathogens. They are capable of translocating an arsenal of specific bacterial toxins (effector proteins) from the prokaryotic cytoplasm across the three biological membranes directly into the eukaryotic cytosol, some of which modulate host cell mechanisms for the benefit of the pathogen. They populate a particular biological niche, which is maintained by specific, pathogen-dependent effectors. In contrast, the needle complex, which is the central component of this specialized protein delivery machine, is structurally well-conserved. It is a large supramolecular cylindrical structure composed of multiple copies of a relatively small subset of proteins, is embedded in the bacterial membranes and protrudes from the pathogen's surface with a needle filament. A central channel traverses the entire needle complex, and serves as a hollow conduit for proteins destined to travel this secretion pathway. In the past few years, there has been a tremendous increase in an understanding on both the structural and the mechanistic level. This review will thus focus on new insights of this remarkable molecular machine.

Keywords: microbial pathogenesis; type-3 secretion; structure; dissection; function; *Salmonella*

1. TYPE-3 SECRETION SYSTEMS ARE COMPLEX SYSTEMS—FROM STRUCTURE TO MECHANISM

Many animal as well as plant pathogens share the same principles to infect host cell organisms: they translocate specific bacterial toxins (collectively called 'effector proteins'), which originate from the bacterial cytoplasm directly into the cytoplasm of a eukaryotic host cell. As a consequence, translocated effector proteins have the remarkable capacity to modulate various host-cell pathways, including endocytic trafficking, gene expression, programmed cell death or cytoskeleton dynamics that induce membrane ruffling and subsequently make the host accessible to bacterial infection [1,2]. At the heart of this process stands the type-3 secretion system (T3SS), a protein-delivery machine, which establishes intimate contact between the micro-organism and the eukaryotic host. It is therefore believed that it allows the safe and unidirectional passage of specific effectors into the host cell. The destination of many effectors is the host cell cytoplasm, the host-cell membrane or the extracellular environment [3,4]. These systems are widespread among Gram-negative animal pathogens, such as *Yersinia*, *Pseudomonas*, *Shigella*, enteropathogenic and enterohaemorrhagic *Escherichia coli* (*EPEC* and *EHEC*, respectively), or *Salmonella*, and the plant pathogens *Erwinia, Ralstonia* or *Xanthomonas*. They are often essential for the onset of a diversity of diseases ranging from diarrhoea, bubonic plague or even fatal outcomes, to fire blight and bacterial wilt, respectively [5]. While, in principle, the task of translocating proteins from one compartment to the other has been solved in nature previously (for example the targeting and/or secretion of proteins through the Sec- or the Tat-system), the contextual situation is complicated: translocation must occur through a number of environments such as the cytosol, the periplasm and the extracellular space. Consequently, the function of a T3SS system is complex in both the specific mechanistic details and the organization of all individual components involved. For simplicity, in this review, we will primarily focus on recent insights obtained on the *Salmonella*-specific T3SS but will add additional information from other systems such as *Shigella* or *Yersinia* for comparison. (Homologous components from various species are listed in table 1.)

2. ACTIVITY OF TYPE-3 SECRETION SYSTEMS DURING INFECTION

The initiating event for many Gram-negative bacterial infections is the activity of the T3SS, which mediates intimate contact between a single bacterium and the eukaryotic host cell (figure 1*a*). In *Salmonella*, this T3SS is encoded on a specific gene cluster (*Salmonella* pathogenicity island (SPI-1); figure 1*b* and table 1) on the bacterial chromosome and translocates effectors during the invasion phase of epithelium cells. The effectors trigger host cellular responses essential for the

* Author for correspondence (marlovits@imp.ac.at).

One contribution of 11 to a Theme Issue 'Bacterial protein secretion comes of age'.

Table 1. Collection of homologous proteins of T3SS from various species. OM, outer membrane; IM, inner membrane.

	Salmonella			*Shigella*			*Yersinia*			*E. coli (EHEC O157:H7)*			
localization	protein	amino acid	accession number	protein	amino acid	accession number	protein	amino acid	accession number	protein	amino acid	accession number	functional component
host cell membrane	SipB	593	AAL21765.1	IpaB	580	ADA76866.1	YopB	401	CAL10037.1	EspD	374	ACG59617.1	translocon
	SipC	409	AAL21764.1	IpaC	363	ADA76865.1	YopD	306	CAL10036.1	EspB	312	ACG59616.1	translocon
extracellular	SipD	343	AAL21763.1	IpaD	332	ADA76864.1	LcrV	324	CAL10039.1	EspA	192	ACG59618.1	needle tip
	PrgI	80	AAL21753.1	MxiH	83	ADA76875.1	YscF	87	CAL10063.1	EscF	73	ACG59614.1	needle filament
OM/ periplasm	InvG	562	AAL21778.1	MxiD	566	ADA76883.1	YscC	607	CAL10060.1	EscC	512	ACG59637.1	secretin/outer ring
	PrgJ	101	AAL21752.1	MxiI	97	ADA76876.1	YscI	115	CAL10066.1	EscI	142	ACT74408.1	inner rod protein
	InvH	147	AAL21780.1	MxiM	142	ADA76881.1	YscW	131	CAL10056.1				assists in secretin insertion into OM
IM	PrgK	252	AAL21751.1	MxiJ	241	ADA76877.1	YscJ	244	CAL10067.1	EscJ	190	ACG59635.1	smaller inner ring protein
	PrgH	392	AAL21754.1	MxiG	371	ADA76874.1	YscD	418	CAL10061.1	EscD	406	ACG59620.1	larger inner ring protein
	SpaP	224	AAL21770.1	Spa24	216	CAC05828.1	YscR	217	CAL10052.1	EscR	217	ACG59645.1	export apparatus
	SpaR	263	AAL21768.1	Spa29	256	CAC05830.1	YscT	261	CAL10054.1	EscT	258	ACG59643.1	export apparatus
	SpaS	356	AAL21767.1	Spa40	342	ADA76894.1	YscU	354	CAL10055.1	EscU	345	ACG59642.1	export apparatus, substrate switching
	InvA	685	AAL21776.1	MxiA	686	AAP79010.1	YscV	704	AAK69216.1	EscV	675	ACG59631.1	export apparatus
	SpaQ	86	AAL21769.1	Spa9	86	ADA76892.1	YscS	88	CAL10053.1	EscS	89	ACG59644.1	export apparatus
cytoplasm	SpaO	303	AAL21771.1	Spa33	293	ADA76890.1	YscQ	307	CAL10051.1	EscQ	305	ACT74401.1	sorting platform
	OrgA	199	AAL21750.1	MxiK	172	ADA76878.1	YscK	209	CAL10068.1	Orf4	109	AAC70125.1	sorting platform
	OrgB	226	AAL21749.1	MxiN	226	ADA76879.1	YscL	223	CAL10069.1	EscL	204	ACT74420.1	sorting platform
	InvC	431	AAL21774.1	Spa47	430	ADA76887.1	YscN	439	CAL10048.1	EscN	446	ACG59630.1	ATPase
indifferent	InvI	147	AAL21773.1	Spa13	112	ADA76888.1	YscO	154	CAL10049.1				?
	InvE	372	AAL21777.1	MxiC	355	AAP79009.1	YopN	293	CAL10047.1	SepL	351	ACG59619.1	regulator translocation
	InvJ	336	AAL21772.1	Spa32	292	ADA76889.1	YscP	453	CAL10050.1	Orf16	138	ACT74402.1	regulator/gatekeeper?
	OrgC	150	AAL21748.1	MxiL	135	ADA76880.1							?

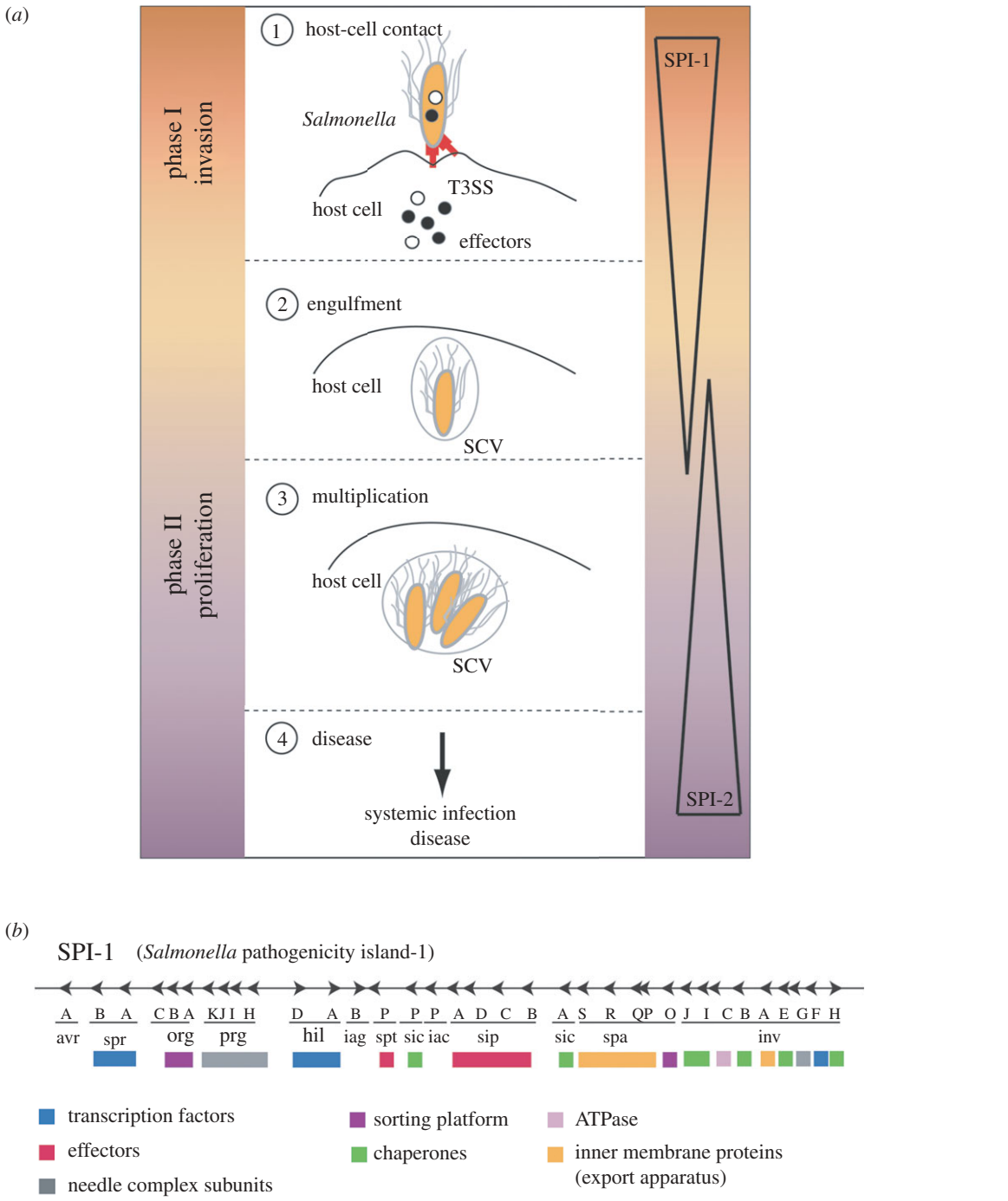

Figure 1. Infection pathway and organization of the T3SS. (*a*) *Salmonella* invasion scheme: (1) during the invasion phase (controlled by the *Salmonella* pathogenicity island 1, SPI-1), a contact between *Salmonella* and the host cell activates the SPI-1-encoded T3SS, which starts to secrete effector proteins that modify the cytoskeleton of the cell. This results in membrane ruffling that facilitates the subsequent uptake of the bacterium and formation of the *Salmonella*-containing vacuoles (SCVs) (2). (3) In the proliferation phase (maintained by SPI-2), the bacterium multiplies inside the SCVs before it is finally released to cause systemic infection (4). (*b*) Genomic organization of the *Salmonella* pathogenicity island-1 (SPI-1) and functional grouping of proteins: transcription factors, effectors, needle complex subunits, sorting platform, chaperones, inner membrane proteins (export apparatus), type-3 specific ATPase.

bacterial pathogenicity [6]; for example, the host cell's actin cytoskeleton network is remodelled and membrane ruffling occurs, which allows the bacteria to be engulfed into non-phagocytic cells. Shortly after internalization, *Salmonella* resides on a membrane-bound compartment similar to early endosomes. However, these compartments segregate from the prototypical endocytotic pathway, avoid fusion with degradative compartments [7] and establish an intracellular replicative niche. The maturation into a replicative environment (SCV, *Salmonella*-containing vacuole) requires the activity of a second T3SS, which is expressed about 3 h post-infection, encoded on a second pathogenicity island (SPI-2; figure 1*a*) [8,9]. Effector proteins modifying the microtubule-associated motor proteins dynein and kinesin furthermore influence the intracellular

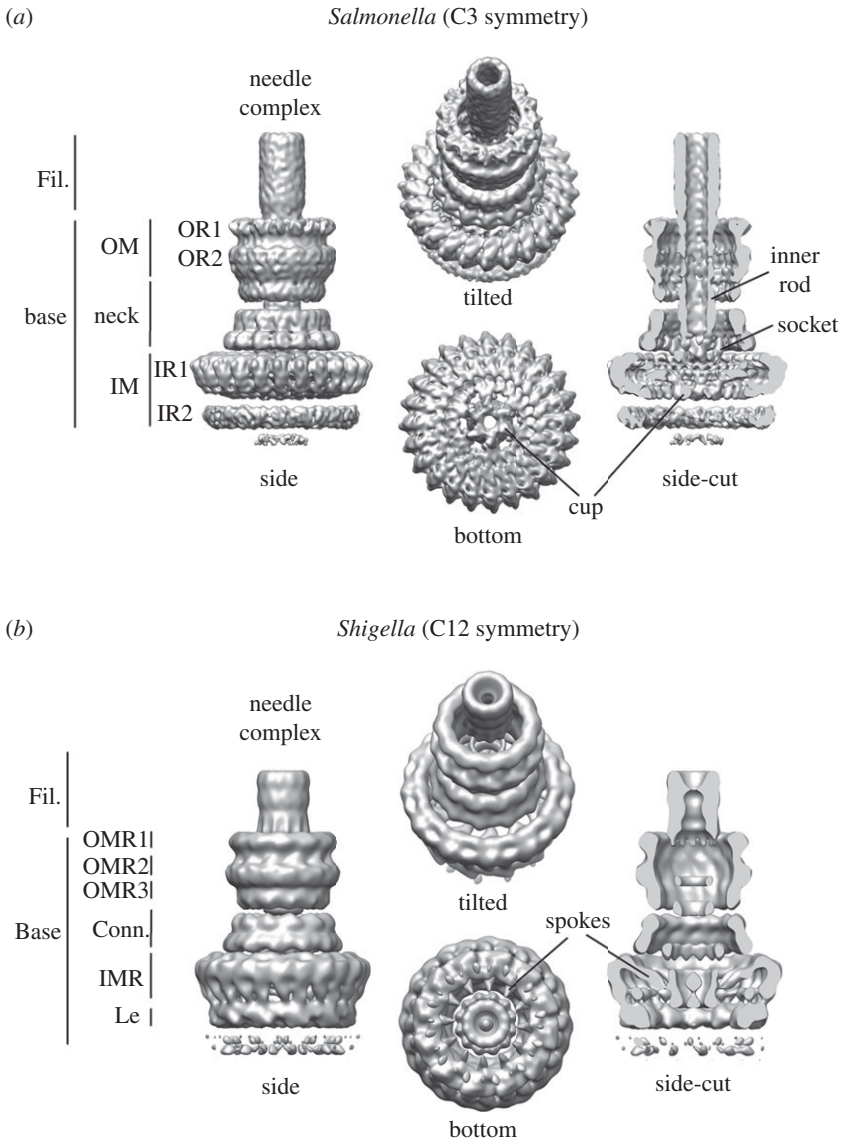

Figure 2. Needle complex structure from (*a*) *Salmonella* and (*b*) *Shigella*. Fil., needle filament; OM, outer membrane; OR, outer ring; OMR, outer membrane ring; IM, inner membrane; IR, inner ring; IMR, inner membrane ring; Conn., connector; Le, leg. Accession code: EMD-1875 (*Salmonella*), EMD-1617 (*Shigella*).

positioning of the SCV leading to a highly associated interaction with the Golgi network and ensure the proper maintenance of the SCV [10–14]. The consecutive action of both SPI-1 and SPI-2 T3SSs allow *Salmonella* not only to invade eukaryotic hosts but also to modify their cell machinery, such that the bacterium becomes able to evade the host's defence mechanism and to replicate and spread in a protected environment (see the study of Coburn *et al.* [1] for a more complete description of T3SS and corresponding diseases). During recent years, most of our understanding about mechanistic insights, including structural information, was obtained from the SPI-1-encoded T3SS, which will be the further focus of this review.

3. THE NEEDLE COMPLEX: THE STRUCTURAL CORE OF TYPE-3 SECRETION SYSTEMS

The core and probably the most prominent structure of the T3SS (SPI-1) is the needle complex (figure 2), a 'syringe'-like multi-component system. It was first visualized from *Salmonella* more than a decade ago [15], and subsequently also from other bacteria, such as *Shigella* [16,17] or *EPEC* [18]. Overall, the needle complex is a large (approx. 30×80 nm), cylindrical complex, which in its native environment is embedded in both the inner (IM) and the outer membrane (OM); it spans the periplasmic space and protrudes into the extracellular environment with a needle filament. Its overall architecture provides a structural framework for a direct connection of the bacterial and host cell cytoplasm and delineates the secretion path through the needle complex. Although the needle complex is about 3.5 MDa in size, its overall shape is dictated by only a relatively small subset of proteins [15]. Over the past few years, we have witnessed a tremendous insight into the overall architecture obtained by nuclear magnetic resonance (NMR) and/or X-ray crystallography for individual proteins, and electron microscopy for assembled needle complexes. While the needle filament is a helical polymer [19,20] of more than 100 individual monomers of a single approximately

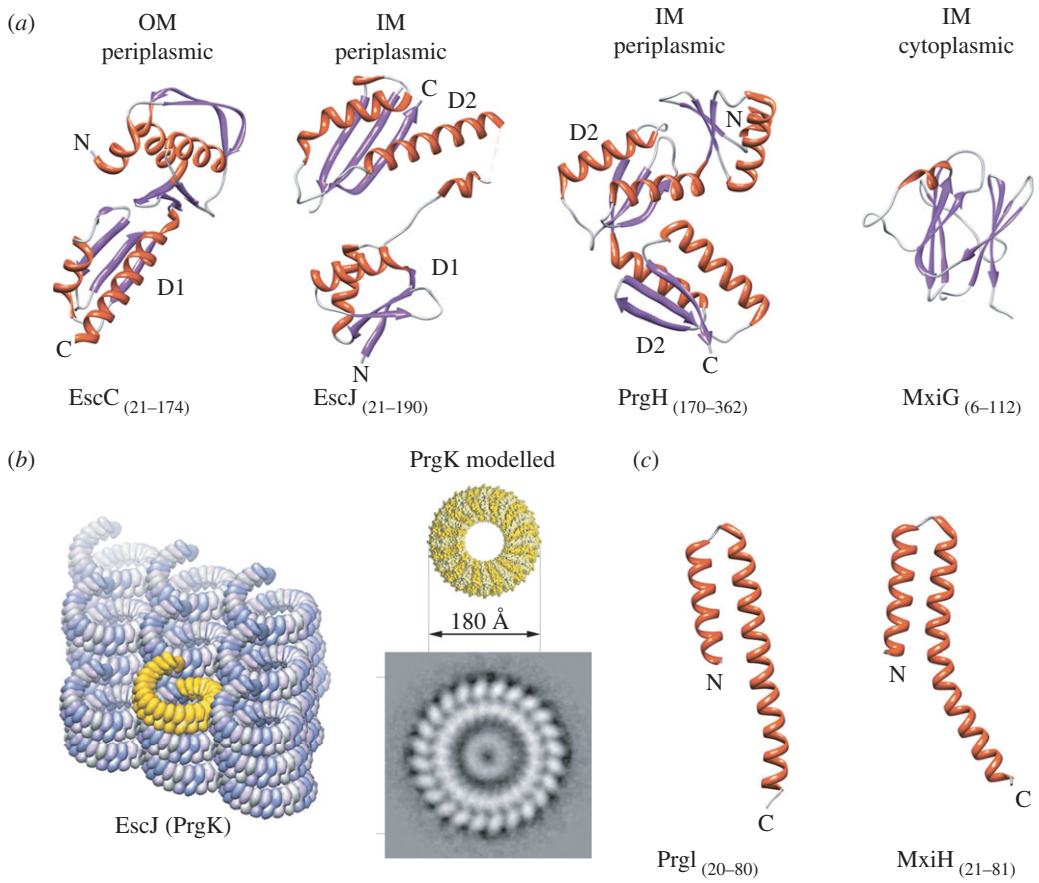

Figure 3. Domain structures of some needle complex proteins. (Summary of T3SS structures solved by X-ray, NMR, EM listed in table 2.) (*a*) Ribbon diagrams of domains of needle complex proteins building up the membrane-embedded base: InvG homologue EscC (X-ray, PDB: 3GR5), PrgK homologue EscJ (X-ray, PDB: 1YJ7), PrgH (C-terminal, periplasmic domain, X-ray, PDB: 3GR0), PrgH homologue MxiG (N-terminal, cytoplasmic domain, NMR, PDB: 2XXS). (OM (outer membrane), IM (inner membrane)). The periplasmic domains are organized into small modules. Domains D1 and D2 were speculated to be conserved ring-building motifs. (*b*) (Left panel) Crystal packing of PrgK homologue EscJ in a superhelix covering 24 subunits per turn (yellow). (Right panel) The modelled PrgK ring (yellow) based on the crystal contacts of EscJ but without helical rise. It displays the same diameters (approx. 180 Å) as the smaller ring of the inner ring obtained by selective disassembly of needle complexes. (*c*) Ribbon diagrams of domains of the needle filament forming proteins: PrgI from *Salmonella* (left) and MxiH in *Shigella* (right) (both X-ray, PDB 2X9C, 2CA5).

10 kDa protein (PrgI), the membrane embedded base is composed of multiple copies of three proteins (InvG, PrgH and PrgK) [15] (figures 1*b* and 3*a*). From the first three-dimensional reconstructions from negatively stained [17] and cryo-electron microscopy images [53] of isolated needle complexes from *Shigella* or *Salmonella*, respectively, it became clear that both bases are organized into several ring-like structures of different diameters, suggesting a close evolutionary relationship between different T3SSs [5,54,55]. More recently, these reconstructions have been significantly improved to 5–10 Å for fully hydrated, vitrified needle complexes from *Salmonella* [21] and to 21–25 Å for negatively stained complexes from *Shigella* [22] (figure 2). In comparison, the overall shape is similar; however, differences are seen at all individual levels. In particular, the highly oligomeric needle complex from *Salmonella* displays a threefold symmetry in which 15 subunits of the OM neck ring connect to 24 subunits of the IM ring (figure 2*a*). Moreover, the reconstruction from approximately 37 000 individual particles from vitrified needle complexes revealed an organization of the cup and socket into individual subunits, which probably defines the entry pathway for substrates, and/or serves as an adaptor to the inner rod/helical filament, respectively. The image analysis also showed that the most rigid substructures are individually resembled by the inner ring/neck and the OM ring, which are flexibly connected at the constriction within the neck. Also, the lower ring, IR2, displays various conformations or compositional differences. The needle complex from *Shigella* was reconstructed from a selected group of 41 negatively stained particles. By applying a 12-fold symmetry, individual subunits were reported throughout the complex [22] (figure 2*b*): For example, the 24 subunits of the inner ring, which are not equally spaced, or the 12 spokes connecting the socket/cup with the IM ring clearly demarcate differences to the needle complex from *Salmonella*. A direct comparison will be possible once the *Shigella* needle complex structure is solved by cryo-electron microscopy and single particle reconstruction.

Recently, needle complexes of *Salmonella* have been selectively disassembled into stable individual rings: the OM ring, which is composed of the OM protein

Table 2. Collection of structures of T3SS proteins. AFM, atomic force microscopy; CBD, chaperone-binding domain; OM, outer membrane; IM, inner membrane; EM, electron microscopy; n.dep., not deposited.

functional component	substructure/ characterized homologues	organism	structural methods	resolution (Å)	Reference	EMDB/PDB
needle complex	needle complex (C3)	*Salmonella*	EM (cryo)	9.5–11.7	[21]	1875
	needle complex (C12)	*Shigella*	EM (neg. stain)	21–25	[22]	1617
	outer ring (C15)	*Salmonella*	EM (cryo)	6.7–8.3	[21]	1871/2Y9K
	inner ring (C24)	*Salmonella*	EM (cryo)	4.7–6.4	[21]	1874/2Y9J
needle filament	filament	*Shigella*	EM (neg. stain)	16	[23]	1416
	filament	*Salmonella*	EM (cryo)	19.5	[19]	n.dep.
ATPase	ATPase (HrcN)	*Pseudomonas*	EM (cryo)	16	[24]	1160
translocon	EspB	*EPEC*	AFM		[25]	n.dep.
	EspD	*EPEC*	AFM		[25]	n.dep.
	$PopD^{CBD}$: PcrH	*Pseudomonas*	X-ray	1.85	[26]	2XCB
	$IpaB^{CBD}$: IpgC	*Shigella*	X-ray	2.15	[27,28]	3GZ1
needle tip	LcrV	*Yersinia*	X-ray	2.17	[29]	1R6F
	IpaD	*Shigella*	X-ray	2.10	[30]	2J0N
	BipD	*Burkholderia*	X-ray	2.60	[31]	2IXR
	EspA : CesA	*EPEC*	X-ray	2.80	[32]	1XOU
needle	PrgI	*Salmonella*	X-ray	2.45	[20]	2X9C
	YscF	*Yersinia*	X-ray	1.80	[33]	2P58
	MxiH	*Shigella*	X-ray	2.10	[34]	2CA5
	BsaL	*Burkholderia*	NMR		[35]	2G0U
	PscF	*Pseudomonas*	X-ray	2.00	[36]	2UWJ
OM—secretin	InvG	*Salmonella*	EM (cryo)	6.7–8.3	[21]	2Y9K
	InvG	*Salmonella*	EM (neg. stain)		[37]	n.dep.
	EscC	*EPEC*	X-ray	2.05	[38]	3GR5
	YscC	*Yersinia*	EM (neg. stain)		[39]	n.dep.
OM—pilotin	MxiM	*Shigella*	X-ray	1.5	[40]	1Y9L
	MxiM : secretin	*Shigella*	NMR		[41]	2JW1
IM proteins	PrgH	*Salmonella*	X-ray	2.3	[38]	3GR0
	PrgH : PrgK	*Salmonella*	EM (cryo)	4.7–6.4	[21]	2Y9J
	EscJ	*EPEC*	X-ray	1.8	[42]	1YJ7
	EscJ	*EPEC*	NMR		[43]	n.dep.
	MxiG	*Shigella*	NMR		[44]	2XXS
export apparatus	InvA	*Salmonella*	X-ray	1.5	[45,46]	2X49
	SpaS	*Salmonella*	X-ray	2.6	[47]	3C01
	EscN	*EPEC*	X-ray	2.25	[48]	2OBM
	EscU	*EPEC*	X-ray	1.5	[47]	3BZT
	YscU	*Yersinia*	X-ray	1.3	[49,50]	2JLJ
	Spa40	*Shigella*	X-ray	2.0	[51]	2VT1
	HrcQ	*Pseudomonas*	X-ray	2.29	[52]	1O9Y
ATPase	EscN	*EPEC*	X-ray	1.8	[48]	2OBM, 2OBL

InvG, and the IM ring, which is constituted by the IM proteins PrgH and PrgK [21,56].

4. THE INNER MEMBRANE PROTEIN RING

The IM ring is composed of two IM proteins (PrgH/PrgK) and represents the largest ring visualized within the needle complex [56]. The first structure of the base complex proteins reported came from NMR experiments of a truncated form of EscJ (PrgK homologue), in which a two-domain structure with a flexible linker was described [43]. Subsequently, a triple mutant of the PrgK-homologue EscJ was crystallized, confirming the two-domain structure [42] (figure 3*a*). Based on the crystal packing, in which 24 monomers arranged in a superhelix in the crystal lattice covered one full helical turn (figure 3*b*), it was speculated that EscJ/PrgK on its own is able to form a ring accommodating 24 monomers, which then also would represent the initial platform for needle complex assembly. As such, a model would predict the formation of an EscJ/PrgK-ring sometime during the assembly process. It will be interesting to see whether such rings can be isolated in future. The dimensions of the proposed modelled ring, however, are smaller than the largest IM dimensions measured from electron microscopy images from side views of isolated complexes, suggesting an additional role of the second protein (PrgH). Recently, it has been possible to obtain an end-on view of IM rings by selective disassembly of previously assembled and isolated needle complexes [21,56]. From this analysis, it became clear that the IM ring is organized into two concentric rings with different diameters (figure 3*b*): the smaller ring matches the proposed and modelled

EscJ ring [42]. This suggests that PrgH and PrgK individually form the two concentric rings, and that the PrgK ring is shielded by embracement of a larger (PrgH) ring together with the lower neck OM on top of IR1. This architecture is also consistent with data obtained by mass spectrometry in which the accessibility of chemical derivatization of PrgK was measured in a mutant complex lacking the OM protein ring InvG [42,56]. Similar to the PrgK ring, the larger PrgH ring clearly shows 24 equally spaced individual subunits [56,57]. The accessibility for chemical derivatization and also nano-gold labelling established that the larger inner ring consists of PrgH monomers [56].

Both PrgH and PrgK display a predicted single alpha-helical transmembrane domain (TM); however, only PrgK harbours a prototypical signal sequence at its N-terminus that is cleaved after membrane insertion. As a consequence, the two proteins are topologically inverted with respect to each other, as has been experimentally shown by specific nano-gold labelling of isolated needle complexes [56]. While the transmembrane domain in PrgH separates the protein into two parts of similar size, PrgK is mainly organized as a large N-terminal domain followed by the TM- and a short C-terminal domain. Taken together, the C-terminal domain of PrgH and the N-terminal domain of PrgK are localized periplasmically, and the N-terminal domain of PrgH and C-terminal domain of PrgK face the bacterial cytoplasm. Within the needle complex, the periplasmically associated IM ring has been referred to as IR1, but the cytoplasmically associated domain as IR2 (figure 2*a*). Recently, the C-terminal domain of PrgH residing in IR1 has been solved to atomic resolution [38]. This domain is organized into a modular arrangement of a repeated pattern (αββαβ (D2-domain)), similar to what has been observed in EscJ. It has been hypothesized that this motif is responsible for ring formation (figure 3*a*). In fact, PrgH contains two D2 domains; however, in contrast to EscJ, it does not crystallize in a helical or ring-like arrangement. Within the cytoplasmic ring IR2, about 140 amino acids of the N-terminal domain of PrgH and 30 amino acids of the C-terminal tail of PrgK are present. The N-terminal PrgH domain is predicted to fold into a forkhead-associated domain (FHA), which was confirmed recently by solving the structure of its homologue from *Shigella* by NMR [44] (figure 3*a*). The FHA domains are known to bind to phosphothreonine peptides in cell-signalling molecules [58]. In the context of T3SS, this would feed an attractive hypothesis for phosphorylation-dependent regulation or modulation of effector protein translocation. However, the putative phosphate-binding pocket neither aligns with the FHA domain nor does it bind phosphothreonine [44]. It is therefore unclear whether this domain plays a regulatory role in using a different unknown mechanism.

5. THE OUTER MEMBRANE PROTEIN RING AND THE NECK

Members of the OM protein belong to the secretin family [59]. This family is characterized by proteins forming higher ordered ring-like structures in the OM of Gram-negative bacteria, where they are required for the assembly of the T3SS and the T2SS [60,61] or extrusion of filamentous phages type IV [62–64]. Secretins are multi-domain proteins that are disposed in a cylindrical arrangement with an open end on both sides. In T3SS, secretins not only form the OM rings but also the neck, which reaches far into the periplasm and docks directly onto IR1 [38,56]. This structure consists of multiple copies of the protein InvG showing 15 subunits [21]. For the *Shigella* needle complex, 12 subunits have been suggested as the most likely configuration [22], and 12–14 for other secretins [60,64–67]. This could indicate that the secretin family has evolved into a ring-forming protein family that is able to adopt different symmetries, probably to optimize their function in the respective systems. It should, however, be noted, that different techniques have been used to measure the number of subunits in the past, and it would be worthwhile to revisit the question of oligomericity within the secretin family using a more systematic and comparable analysis.

The only atomic structure of type-3 secretin (InvG) available is from the first two domains of the homologue EscC [38] (figure 3*a*). In addition, the structure of three domains of GspD, a secretin present in the type-2 secretion system has also been reported recently [68]. Despite the lack of sequence identity, the N-terminal domain of EscC shows structural similarity to the first domain (D1) of EscJ/PrgK with a βαββα-fold, and as such has been speculated to be a conserved ring-forming motif [38]. However, the D1 domain is also present in systems that do not form higher oligomeric rings, such as phage systems that bind peptidoglycan or in eukaryotic RNA and DNA KH domains [69,70]. This indicates that this domain has been functionally exploited by other systems. It is therefore still under debate whether the structural motif present is sufficient and/or necessary to form ring-like structures.

6. THE EXTRACELLULAR COMPONENTS: THE NEEDLE FILAMENT, THE TIP AND THE TRANSLOCON

The most prominent extracellular component of the T3SS is the needle filament [17,71–73], which protrudes from the bacterial OM and consequently establishes an extracellular 'secretion tunnel' to the host cell. The helical needle is built up of more than 100 copies [74] of a small protein (PrgI/YscF/MxiH (*Salmonella*/*Yersinia*/*Shigella*) <10 kDa). Native needles have a typical length varying from 30 to 70 nm and an outer diameter of about 10–13 nm [20,23,75]. Assembly of the needle filament requires first the transport to and then the polymerization of individual monomers at the distal end of the complex. While the transport requires the activity of the T3-specific ATPase (InvC), which presumably unfolds PrgI monomers like other T3-substrates [76], the polymerization itself is ATP-independent and occurs in two distinct steps: nucleation and elongation [77]. During this process, needle subunits have to be refolded [20]. The helical parameters of the assembled needle vary from 5.6 subunits per

turn in *Shigella* [23] to 6.3 in *Salmonella* [19]. The length of the growing needle filament is under the control of another component (InvJ (*Salmonella*), Spa32 (*Shigella*), or YscP (*Yersinia*)) [72,75,78–80]; however, the precise mechanism of needle length control is under debate [81]. A recently published structure of truncated PrgI showed that the soluble monomer comprises a helical core and flexible termini (Asp11–Thr18 and Gln61–Asn78) [20]. Starting from Gly19 to the C-terminus, PrgI adopts an α-helical hairpin conformation (as shown by X-ray crystallography; figure 3*c*) which, according to the NMR studies, is further extended from Asp11 to Thr18. Additionally, both structures indicate that the C-terminus of the unpolymerized protein is α-helical but changes its conformation into two extended strands upon assembly. The MxiH (*Shigella*) monomer adopts a similar fold [34] (figure 3*c*), and revealed two long α-helices, connected by a Pro-Ser-Asn-Pro turn. The first helix can further be divided into a head and a tail region. NMR and mutational studies showed that this turn together with the head region are involved in the MxiH interaction with the tip protein IpaD [34,82]. By positioning the crystal structure of a monomeric MxiH into a previously generated electron microscopy density map, a model was generated in which the N-terminal helix of MxiH is facing the inner channel of the filament, while the C-terminal one is suspected to be involved in its assembly [23,34].

The T3SS needle filament ends distally in the so-called tip complex formed by multiple copies of an adaptor protein SipD (*Salmonella*) [83–86], and is involved in regulating the secretion process as well as positioning onto the translocation pore in the host cell membrane [87–91]. The structure of SipD has been solved recently [28,92] and shown to be predominantly α-helical, and can be divided into three structurally distinct domains: the N-terminal self-chaperoning domain-1 that impedes the interaction and comprises two α helices, the central domain-2 that adopts a coiled-coil structure with two helices (47 and 52 amino acids in length), linked to domain-3 showing a mixed α/β-structure. The latter two domains mediate binding of SipD to PrgI, as demonstrated by isothermic titration calorimetry [28]. To better understand the interaction of needle filament monomers (PrgI) and tip proteins (SipD), the structure of SipD fused to PrgI was solved. Subsequently, a pentameric tip-complex was modelled *in silico*, which could represent the configuration that interacts with the bacterially deployed translocon proteins that presumably form a pore-like structure for the passage of T3 effectors through the eukaryotic host cell membrane. Tip (SipD) and translocon (SipB, SipC) are essential for the intimate contact between bacteria and host cells and have been speculated to play an important role in host-sensing and activation of late T3 effector protein secretion [83,84,93,94]. However, the underlying mechanistic details are still to be uncovered.

7. THE BLUEPRINT OF THE NEEDLE COMPLEX TO SUB-NANOMETRE RESOLUTION

A big step forward in the understanding of the architecture of the needle complex came from the first electron microscopy reconstruction of isolated needle complexes a few years ago [22,53]. At low resolution (17 and 25 Å, respectively), the organization of the base in a series of rings could be depicted, new structural elements, such as the inner rod, the socket and the cup were identified for the first time [53]. However, profound differences, such as the 'spokes' in the *Shigella* needle complex, which are not present in complexes of *Salmonella* were described [22]. At this low resolution, conformational changes have been recognized as they occur during the assembly from the base to the fully assembled needle complex [53]. This indicates that the underlying building blocks (PrgH, PrgK, InvG) must be organized in a way that guarantees stability to maintain a structural scaffold, and sufficient flexibility as required during assembly at the same time. However, subsequent attempts to 'dock' the previously obtained atomic structures from the individual proteins into the context of the needle complex allowed at best a rough positioning [22,38,56,95]. As a result, a series of incompatible models with ambiguous placement of protein domains was reported. Most recently, the structure of the needle complex from *Salmonella* has been solved to sub-nanometre resolution by cryo-electron microscopy and single-particle analysis [21]. At such a resolution (5–10 Å), fine details, such as alpha helices, became visible and precise docking could be performed. As indicated from the analysis of oligomericity of the individual rings, which showed 15 subunits of the outer ring/neck and 24 subunits of the inner ring it was suggested that the entire needle complex displays an overall three-fold symmetry. This would imply that a local symmetry mismatch exists, in which five of the OR/neck subunits are positioned over eight IR1 subunits. In fact, a threefold symmetry of entire needle complexes (figure 2*a*) could be elegantly demonstrated by a change in the observation angle of complexes [21]: as the preferential side-view orientation of the particles on the electron microscopy grid precludes a thorough symmetry analysis, the particle orientation was changed to end-on views by modulating the protonation state of polyhistidine tags introduced in PrgH.

Symmetrization over the asymmetric unit within the individual rings allowed the resolution in these regions to be increased further (figure 4*a*). Subsequent docking revealed the precise organization of individual proteins within and between the individual rings in the context of the needle complex: the periplasmic IR1 is composed of the two individual concentric rings established by C-terminal PrgH (larger ring) and N-terminal PrgK domains (smaller ring), both of which harbour 24 monomers within each ring (figure 4*b,c*). On top of IR1 the 'lower neck' associates; this is composed of 15 monomers of the N-terminal domain of InvG (figure 4*d*). The close interaction between these two rings was further independently confirmed by cross-linking and mass spectrometry experiments as well as by mutational analysis [56,95]. Interestingly, the last 30 amino acids in PrgH are not structured in a crystal, indicating that the C-terminal tail confers some flexibility [38]. Such flexibility might in fact be necessary during the assembly, in which the neck undergoes

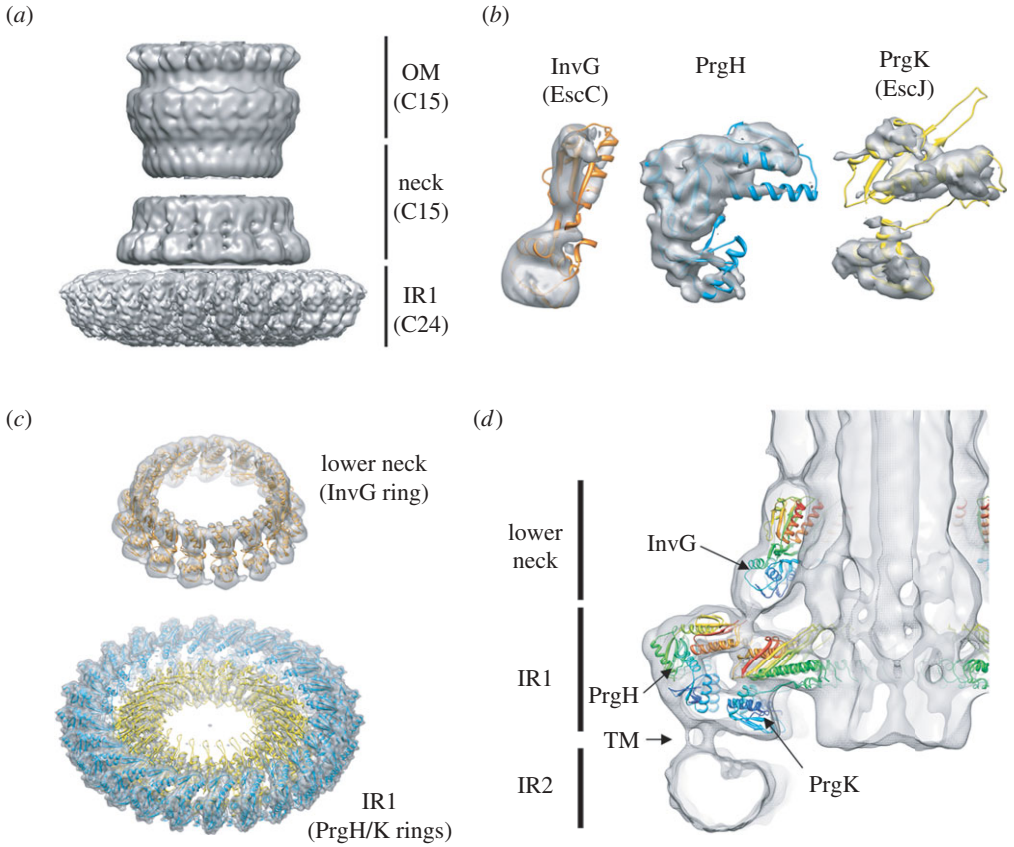

Figure 4. The structure of the needle complex at subnanometre resolution and docking of individual proteins. (*a*) Three-dimensional surface view of the *Salmonella*'s needle complex. As different symmetries are present in the IR1 (24-fold) and OM/neck region (15-fold), symmetrization led to higher resolutions. (*b*) InvG (orange), PrgH (blue) and PrgK (yellow) were independently docked into the three-dimensional cryo-electron microscopy map of the needle complex as rigid bodies guided by their domain structure and secondary elements. (*c*) Fifteen monomers of InvG and 24 of PrgH/PrgK were docked into the lower neck ring and IR1, respectively. PrgH and PrgK are organized as concentric rings with different diameters. (*d*) A slice through the needle complex (side view) with docked atomic structures shows the organization of all three proteins—InvG, PrgH and PrgK—within the needle complex. Tube-like densities, which most probably correspond to the TM helices of PrgH and PrgK, connect IR1 with IR2 and define the localization of the inner membrane bilayer. Accession code: EMD-1874 and PDB 2Y9J (IR1), EMD-1871 and PDB 2Y9K (OM neck), EMD-1875 (needle complex)

large conformational changes by moving outwards in order to accommodate the inner rod [53]. Moreover, the C-terminal tail of PrgH, is required for the stability of the complex, as removing the last four amino acids causes the complex to be less stable [56]. Removal of six amino acids already led to strains that are not able to secrete effectors [95], most probably because of the lack of formation of complexes.

While overall IR1 appears rather rigid in needle complexes, the cytoplasmic IR2 is very flexible. It is possible that this flexibility might occur because of a rather loose transmembrane connection to IR1 in solubilized complexes and is decreased when present in its native membrane environment. A subsequent prerequisite for a precise docking of the N-terminal PrgH FHA domain, modelled based on the recently solved PrgH homologue MxiG from *Shigella* [44], within the IR2 of the *Salmonella* needle complex would, however, require an improved map of that particular region, which eventually could be obtained, for example, by increasing the rigidity of this region.

Electron microscopic analysis also revealed a likely configuration of the socket and the cup in individual subunits. This structure has been associated with a group of highly conserved membrane proteins (SpaP, SpaQ, SpaR, SpaS, InvA in the case of *Salmonella*) [96], which have been collectively called the 'export apparatus'. These proteins have been shown to play an essential role during the assembly into functional needle complexes. Although cytoplasmic domains of InvA [45,46] and SpaS [47] have been solved crystallographically, additional information about stoichiometry and localization of the individual export apparatus proteins is required to define precisely their organization within the needle complex.

8. ASSEMBLY OF THE INJECTISOME

Assembly of the approximately 3.5 MDa needle complex is a highly regulated and coordinated process. Currently, two models have been put forward that originate from studies in the *Yersinia* and *Salmonella* systems: the outside-in and the inside-out model, respectively [96,97]. Both models are characterized by two phases: the early phase (ring formation) is independent of the functional activity of the type-3 specific ATPase, YscN (*Yersinia*) and InvC (*Salmonella*), whereas the successful completion of the subsequent phase (inner rod/filament formation) depends on the ATPase activity.

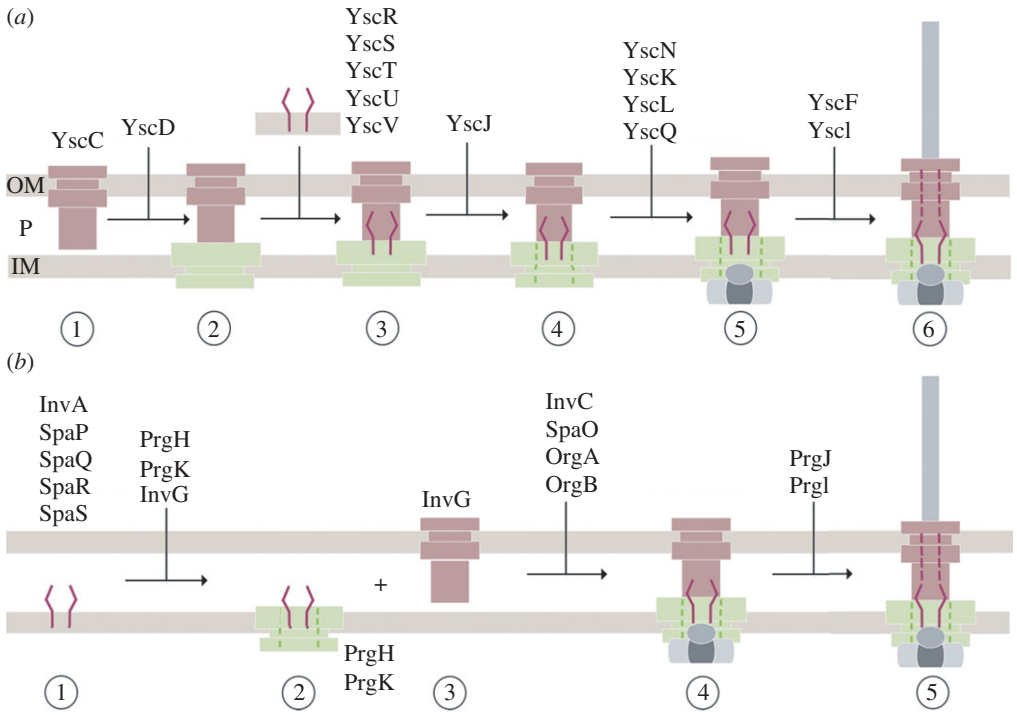

Figure 5. Models of sequential needle complex assembly: (*a*) outside-in model (*Yersinia*) (*b*) inside-out model (*Salmonella*). OM, outer membrane; P, periplasm; IM, inner membrane.

In the outside-in model (*Yersinia*) (figure 5*a*) [97,98], the formation of the needle complex is initiated by the formation of the secretin ring (YscC) in the OM. Subsequently, the IM protein YscD (PrgH homologue and larger ring of the IM ring) associates with the secretin ring. In parallel, the essential export apparatus proteins YscR, YscS, YscT, YscU and YscV, which are believed later to recognize export substrates [99], oligomerize independently. Together, these two substructures recruit YscJ (PrgK homologue) monomers, presumably by sequential attachment to form the smaller IM ring. The ATPase (YscN) and the C ring (YscK, YscL, YscQ) complex assemble synchronously on the cytoplasmic side of the needle complex. In this model, the export apparatus proteins must somehow diffuse laterally into the larger IM ring to integrate to the central part of the needle complex. It is, however, also possible that such an integration could be directly performed co-translationally, which then requires a precise targeting of export apparatus translating ribosomes to the needle complex. In order to finalize the assembly, the ATPase activity is required for the transport of substrates, such as the needle filament and needle-tip proteins.

In the inside-out model (*Salmonella*) (figure 5*b*) [96], assembly nucleates with the export apparatus, which is intimately associated with the needle complex and is composed of a set of conserved membrane proteins (InvA, SpaP, SpaQ, SpaR and SpaS) [96]. In particular, in this model the assembly is initiated first by the formation of a nucleation complex of the two export apparatus proteins SpaP and SpaR. Subsequently, the other two export apparatus proteins SpaQ and SpaS bind to the nucleation complex. Then, multiple copies of the IM proteins PrgH and PrgK as well as the OM protein InvG organize as rings laterally in their respective membrane to form the base of the needle complex. Interestingly, formation into a base-like structure lacking the export apparatus proteins has been shown to be possible [96], suggesting that the underlying ring-forming building blocks have the capability to establish a membrane-embedded complex. The lack of export apparatus proteins yielded complexes devoid of the socket/cup substructure with an overall decreased stability. In addition, the assembly stalls at a base-like complex, demonstrating that the export apparatus proteins are responsible for both the stability of the complex and the assembly into functional needle complexes. Wild-type bases are then traversed by an inner rod (PrgJ) and extended with an extracellular helical needle filament (PrgI) to build up a 25–30 Å wide conduit for protein transport into a later assembly phase [53]. The transport of PrgJ and PrgI monomers is dependent upon and intimately connected to the ATPase activity of InvC [100]. Completion of PrgJ and PrgI transport and incorporation into the needle complex correlates with both large conformational changes observed in the base [53] and with a change in the substrate specificity from secreting the structural proteins (PrgI and PrgJ) to the translocon and effector proteins.

9. SUBSTRATE SECRETION—TIMING, REGULATION AND MECHANISMS

Substrate secretion is a highly orchestrated process in T3SSs. It occurs at various stages during the lifetime of the system, and substrates are secreted in a sequential order. We therefore refer to ‘early’ (inner rod/filament), ‘mid’ (translocases) and ‘late’ (effectors) substrates (figure 6). In *Salmonella*, the early substrates are the structural sub-component proteins PrgJ and

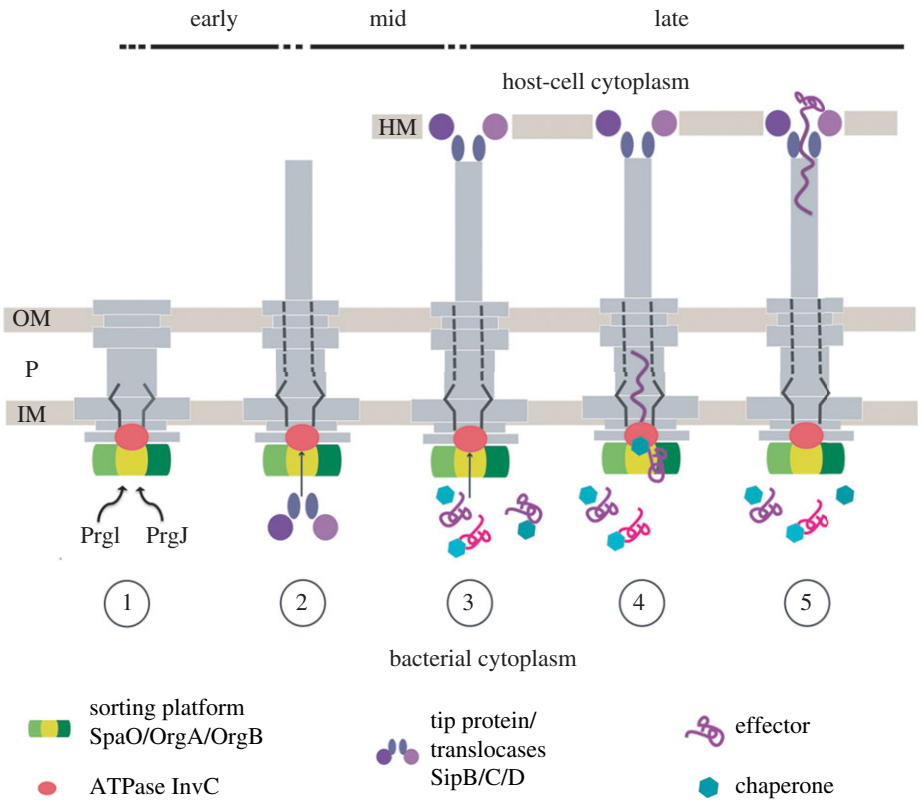

Figure 6. Hierarchy and timing of substrate secretion. (1) In the early phase, PrgI and PrgJ are translocated to build up the inner rod and needle filament; (2) then the translocases are secreted to form the tip (SipD) at the distal end of the needle filament, which connects to the host cell membrane-embedded translocon (SipB, SipC) and establishes a physical connection between the bacterium and the host cell. (3) The effector proteins (late substrates) are translocated from the bacterial to the eukaryotic cytoplasm. Assisted by their cognate chaperones, they interact with the sorting platform (SpaO, OrgA and OrgB) and are then specifically recognized by the T3-associated ATPase (InvC). (4) ATP binding and hydrolysis are required to release the chaperone from its substrate and to unfold the substrate. The unfolded substrate is then believed to travel the secretion pathway through the inner rod and the needle filament (5) into the host cell cytoplasm. OM, outer membrane; P, periplasm; IM, inner membrane; HM, host cell membrane.

PrgI, which form the inner rod and the helical filament structure of the needle complex. In order to establish a physical connection for protein translocation from the bacterial to the eukaryotic cytoplasm, the mid-substrates, SipD, SipB and SipC, are transported. They constitute the needle tip and a pore-like translocon which is embedded in the eukaryotic host cell membrane [101]. This guarantees that late substrates (effectors) are safely translocated directly from the bacterial to the eukaryotic cytoplasm through a number of hostile environments (inner and outer bacterial membrane, periplasmic and extracellular space, host cell membrane). While the recognition of being a type-3 substrate is not fully understood in detail, many substrates, require the coexistence with a cognate chaperone. In *Salmonella*, for example, the effector protein SptP harbours an N-terminal domain of approximately 160 amino acids, which binds the acidic chaperone SicP with nanomolar affinities. Recent studies have shown that a high molecular weight complex of the cytoplasmic proteins SpaO/OrgA/OrgB forms independently of the presence of needle complexes [96]. This complex appears to serve as a binding platform for substrates destined to be translocated via the needle complex, as chaperone–effector complexes bind via the chaperone to this platform. SpaO/OrgA/OrgB also functions as a sorting platform probably through different affinities of various chaperone–effector complexes and thus determines the order of secreted effectors. As only effector proteins but not chaperones are secreted, the latter are released through the activity of the ATPase (InvC). From *in vitro* assays, it has been shown that ATP binding and ATP hydrolysis are not only required to dissociate chaperones from effectors but also to further unfold the effector proteins as they can only be secreted in an at least partially unfolded state. The proton motive force has been implied in substrate transport of T3SSs [102]; the precise mechanism, however, remains elusive [103].

10. CONCLUSIONS

T3SSs are one of the most exciting discoveries over the past couple of years in the field of bacterial pathogenesis. Their efficient and conserved central role in the physical interaction of many pathogenic bacteria and their hosts opens up the possibility for therapeutic intervention. A prerequisite, however, is a detailed knowledge about mechanistic and structural details. The complex nature of the multi-component system which assembles into supramolecular structures requires an integrated analytical approach. While conventional structural technologies (X-ray and NMR)

were highly successful in obtaining atomic details of individual components of the system, cryo-electron microscopy allowed us to bring these pieces together and draw the blueprint of the core component at high precision. Although a few grey areas are still to be explored, the T3SS and the blueprint of the needle complex may already be used to develop novel strategies to prevent bacterial infections.

We would like to thank members of the Marlovits laboratory for their comments on this manuscript. L.K. received funding through a predoctoral Boehringer Ingelheim Fonds fellowship. Research in the Marlovits laboratory is supported from the ZIT (Center for Innovation and Technology, City of Vienna, Austria, Grant: CMCN-V Center for Molecular and Cellular Nanostructure Vienna), from the Research Institute of Molecular Biotechnology of the Austrian Academy of Sciences (IMBA) and from the Research Institute of Molecular Pathology (IMP).

REFERENCES

1 Coburn, B., Sekirov, I. & Finlay, B. B. 2007 Type III secretion systems and disease. *Clin. Microbiol. Rev.* **20**, 535–549. (doi:10.1128/CMR.00013-07)
2 Galan, J. E. 2001 *Salmonella* interactions with host cells: type III secretion at work. *Annu. Rev. Cell Dev. Biol.* **17**, 53–86. (doi:10.1146/annurev.cellbio.17.1.53)
3 Akopyan, K., Edgren, T., Wang-Edgren, H., Rosqvist, R., Fahlgren, A., Wolf-Watz, H. & Fallman, M. 2011 Translocation of surface-localized effectors in type III secretion. *Proc. Natl Acad. Sci. USA* **108**, 1639–1644. (doi:10.1073/pnas.1013888108)
4 Galan, J. E. & Wolf-Watz, H. 2006 Protein delivery into eukaryotic cells by type III secretion machines. *Nature* **444**, 567–573. (doi:10.1038/nature05272)
5 Hueck, C. J. 1998 Type III protein secretion systems in bacterial pathogens of animals and plants. *Microbiol. Mol. Biol. Rev.* **62**, 379–433.
6 Galan, J. E. 1996 Molecular genetic bases of *Salmonella* entry into host cells. *Mol. Microbiol.* **20**, 263–271. (doi:10.1111/j.1365-2958.1996.tb02615.x)
7 Hernandez, L. D., Hueffer, K., Wenk, M. R. & Galan, J. E. 2004 *Salmonella* modulates vesicular traffic by altering phosphoinositide metabolism. *Science* **304**, 1805–1807. (doi:10.1126/science.1098188)
8 Ochman, H., Soncini, F. C., Solomon, F. & Groisman, E. A. 1996 Identification of a pathogenicity island required for *Salmonella* survival in host cells. *Proc. Natl Acad. Sci. USA* **93**, 7800–7804. (doi:10.1073/pnas.93.15.7800)
9 Shea, J. E., Hensel, M., Gleeson, C. & Holden, D. W. 1996 Identification of a virulence locus encoding a second type III secretion system in *Salmonella typhimurium*. *Proc. Natl Acad. Sci. USA* **93**, 2593–2597. (doi:10.1073/pnas.93.6.2593)
10 Boucrot, E., Beuzon, C. R., Holden, D. W., Gorvel, J. P. & Meresse, S. 2003 *Salmonella typhimurium* SifA effector protein requires its membrane-anchoring C-terminal hexapeptide for its biological function. *J. Biol. Chem.* **278**, 14 196–14 202.
11 Deiwick, J. *et al.* 2006 The translocated *Salmonella* effector proteins SseF and SseG interact and are required to establish an intracellular replication niche. *Infect Immun.* **74**, 6965–6972. (doi:10.1128/IAI.00648-06)
12 Guignot, J., Caron, E., Beuzon, C., Bucci, C., Kagan, J., Roy, C. & Holden, D. W. 2004 Microtubule motors control membrane dynamics of *Salmonella*-containing vacuoles. *J. Cell. Sci.* **117**, 1033–1045. (doi:10.1242/jcs.00949)
13 Harrison, R. E., Brumell, J. H., Khandani, A., Bucci, C., Scott, C. C., Jiang, X., Finlay, B. B. & Grinstein, S. 2004 *Salmonella* impairs RILP recruitment to Rab7 during maturation of invasion vacuoles. *Mol. Biol. Cell.* **15**, 3146–3154. (doi:10.1091/mbc.E04-02-0092)
14 Salcedo, S. P. & Holden, D. W. 2003 SseG, a virulence protein that targets *Salmonella* to the Golgi network. *EMBO J.* **22**, 5003–5014. (doi:10.1093/emboj/cdg517)
15 Kubori, T., Matsushima, Y., Nakamura, D., Uralil, J., Lara-Tejero, M., Sukhan, A., Galan, J. E. & Aizawa, S. I. 1998 Supramolecular structure of the *Salmonella typhimurium* type III protein secretion system. *Science* **280**, 602–605. (doi:10.1126/science.280.5363.602)
16 Blocker, A., Gounon, P., Larquet, E., Niebuhr, K., Cabiaux, V., Parsot, C. & Sansonetti, P. 1999 The tripartite type III secreton of *Shigella flexneri* inserts IpaB and IpaC into host membranes. *J. Cell. Biol.* **147**, 683–693. (doi:10.1083/jcb.147.3.683)
17 Blocker, A., Jouihri, N., Larquet, E., Gounon, P., Ebel, F., Parsot, C., Sansonetti, P. & Allaoui, A. 2001 Structure and composition of the *Shigella flexneri* 'needle complex', a part of its type III secreton. *Mol. Microbiol.* **39**, 652–663. (doi:10.1046/j.1365-2958.2001.02200.x)
18 Sekiya, K., Ohishi, M., Ogino, T., Tamano, K., Sasakawa, C. & Abe, A. 2001 Supermolecular structure of the enteropathogenic *Escherichia coli* type III secretion system and its direct interaction with the EspA-sheath-like structure. *Proc. Natl Acad. Sci. USA* **98**, 11 638–11 643.
19 Galkin, V. E., Schmied, W. H., Schraidt, O., Marlovits, T. C. & Egelman, E. H. 2010 The structure of the *Salmonella typhimurium* type III secretion system needle shows divergence from the flagellar system. *J. Mol. Biol.* **396**, 1392–1397. (doi:10.1016/j.jmb.2010.01.001)
20 Poyraz, O. *et al.* 2010 Protein refolding is required for assembly of the type three secretion needle. *Nat. Struct. Mol. Biol.* **17**, 788–792. (doi:10.1038/nsmb.1822)
21 Schraidt, O. & Marlovits, T. C. 2011 Three-dimensional model of *Salmonella*'s needle complex at subnanometer resolution. *Science* **331**, 1192–1195. (doi:10.1126/science.1199358)
22 Hodgkinson, J. L. *et al.* 2009 Three-dimensional reconstruction of the *Shigella* T3SS transmembrane regions reveals 12-fold symmetry and novel features throughout. *Nat. Struct. Mol. Biol.* **16**, 477–485. (doi:10.1038/nsmb.1599)
23 Cordes, F. S., Komoriya, K., Larquet, E., Yang, S., Egelman, E. H., Blocker, A. & Lea, S. M. 2003 Helical structure of the needle of the type III secretion system of *Shigella flexneri*. *J. Biol. Chem.* **278**, 17 103–17 107.
24 Muller, S. A., Pozidis, C., Stone, R., Meesters, C., Chami, M., Engel, A., Economou, A. & Stahlberg, H. 2006 Double hexameric ring assembly of the type III protein translocase ATPase HrcN. *Mol. Microbiol.* **61**, 119–125. (doi:10.1111/j.1365-2958.2006.05219.x)
25 Ide, T., Laarmann, S., Greune, L., Schillers, H., Oberleithner, H. & Schmidt, M. A. 2001 Characterization of translocation pores inserted into plasma membranes by type III-secreted Esp proteins of enteropathogenic *Escherichia coli*. *Cell Microbiol.* **3**, 669–679. (doi:10.1046/j.1462-5822.2001.00146.x)
26 Job, V., Mattei, P. J., Lemaire, D., Attree, I. & Dessen, A. 2010 Structural basis of chaperone recognition of type III secretion system minor translocator proteins. *J. Biol. Chem.* **285**, 23 224–23 232.
27 Lokareddy, R. K., Lunelli, M., Eilers, B., Wolter, V. & Kolbe, M. 2010 Combination of two separate binding domains defines stoichiometry between type III

secretion system chaperone IpgC and translocator protein IpaB. *J. Biol. Chem.* **285**, 39 965–39 975.
28 Lunelli, M., Hurwitz, R., Lambers, J. & Kolbe, M. 2011 Crystal structure of PrgI-SipD: insight into a secretion competent state of the type three secretion system needle tip and its interaction with host ligands. *PLoS Pathog.* **7**, e1002163. (doi:10.1371/journal.ppat.1002163)
29 Derewenda, U., Mateja, A., Devedjiev, Y., Routzahn, K. M., Evdokimov, A. G., Derewenda, Z. S. & Waugh, D. S. 2004 The structure of *Yersinia pestis* V-antigen, an essential virulence factor and mediator of immunity against plague. *Structure* **12**, 301–306.
30 Johnson, S. *et al.* 2007 Self-chaperoning of the type III secretion system needle tip proteins IpaD and BipD. *J. Biol. Chem.* **282**, 4035–4044. (doi:10.1074/jbc.M607945200)
31 Pal, M., Erskine, P. T., Gill, R. S., Wood, S. P. & Cooper, J. B. 2010 Near-atomic resolution analysis of BipD, a component of the type III secretion system of *Burkholderia pseudomallei*. *Acta Crystallogr. Sect. F Struct. Biol. Cryst. Commun.* **66**, 990–993. (doi:10.1107/S1744309110026333)
32 Yip, C. K., Finlay, B. B. & Strynadka, N. C. 2005 Structural characterization of a type III secretion system filament protein in complex with its chaperone. *Nat. Struct. Mol. Biol.* **12**, 75–81. (doi:10.1038/nsmb879)
33 Sun, P., Tropea, J. E., Austin, B. P., Cherry, S. & Waugh, D. S. 2008 Structural characterization of the *Yersinia pestis* type III secretion system needle protein YscF in complex with its heterodimeric chaperone YscE/YscG. *J. Mol. Biol.* **377**, 819–830. (doi:10.1016/j.jmb.2007.12.067)
34 Deane, J. E. *et al.* 2006 Molecular model of a type III secretion system needle: implications for host-cell sensing. *Proc. Natl Acad. Sci. USA* **103**, 12 529–12 533. (doi:10.1073/pnas.0602689103)
35 Zhang, L., Wang, Y., Picking, W. L., Picking, W. D. & De Guzman, R. N. 2006 Solution structure of monomeric BsaL, the type III secretion needle protein of *Burkholderia pseudomallei*. *J. Mol. Biol.* **359**, 322–330. (doi:10.1016/j.jmb.2006.03.028)
36 Quinaud, M., Ple, S., Job, V., Contreras-Martel, C., Simorre, J. P., Attree, I. & Dessen, A. 2007 Structure of the heterotrimeric complex that regulates type III secretion needle formation. *Proc. Natl Acad. Sci. USA* **104**, 7803–7808. (doi:10.1073/pnas.0610098104)
37 Crago, A. M. & Koronakis, V. 1998 *Salmonella* InvG forms a ring-like multimer that requires the InvH lipoprotein for outer membrane localization. *Mol. Microbiol.* **30**, 47–56. (doi:10.1046/j.1365-2958.1998.01036.x)
38 Spreter, T. *et al.* 2009 A conserved structural motif mediates formation of the periplasmic rings in the type III secretion system. *Nat. Struct. Mol. Biol.* **16**, 468–476. (doi:10.1038/nsmb.1603)
39 Burghout, P., van Boxtel, R., Van Gelder, P., Ringler, P., Muller, S. A., Tommassen, J. & Koster, M. 2004 Structure and electrophysiological properties of the YscC secretin from the type III secretion system of *Yersinia enterocolitica*. *J. Bacteriol.* **186**, 4645–4654. (doi:10.1128/JB.186.14.4645-4654.2004)
40 Lario, P. I., Pfuetzner, R. A., Frey, E. A., Creagh, L., Haynes, C., Maurelli, A. T. & Strynadka, N. C. 2005 Structure and biochemical analysis of a secretin pilot protein. *EMBO J.* **24**, 1111–1121. (doi:10.1038/sj.emboj.7600610)
41 Okon, M., Moraes, T. F., Lario, P. I., Creagh, A. L., Haynes, C. A., Strynadka, N. C. & McIntosh, L. P. 2008 Structural characterization of the type-III pilot-secretin complex from *Shigella flexneri*. *Structure* **16**, 1544–1554. (doi:10.1016/j.str.2008.08.006)
42 Yip, C. K. *et al.* 2005 Structural characterization of the molecular platform for type III secretion system assembly. *Nature* **435**, 702–707. (doi:10.1038/nature03554)
43 Crepin, V. F., Prasannan, S., Shaw, R. K., Wilson, R. K., Creasey, E., Abe, C. M., Knutton, S., Frankel, G. & Matthews, S. 2005 Structural and functional studies of the enteropathogenic *Escherichia coli* type III needle complex protein EscJ. *Mol. Microbiol.* **55**, 1658–1670. (doi:10.1111/j.1365-2958.2005.04508.x)
44 McDowell, M. A., Johnson, S., Deane, J. E., Cheung, M., Roehrich, A. D., Blocker, A. J., McDonnell, J. M. & Lea, S. M. 2011 Structural and functional studies on the N-terminal domain of the *Shigella* type III secretion protein MxiG. *J. Biol. Chem.* **286**, 30 606–30 614.
45 Lilic, M., Quezada, C. M. & Stebbins, C. E. 2010 A conserved domain in type III secretion links the cytoplasmic domain of InvA to elements of the basal body. *Acta Crystallogr. D Biol. Crystallogr.* **66**, 709–713. (doi:10.1107/S0907444910010796)
46 Worrall, L. J., Vuckovic, M. & Strynadka, N. C. 2010 Crystal structure of the C-terminal domain of the *Salmonella* type III secretion system export apparatus protein InvA. *Protein Sci.* **19**, 1091–1096. (doi:10.1002/pro.382)
47 Zarivach, R., Deng, W., Vuckovic, M., Felise, H. B., Nguyen, H. V., Miller, S. I., Finlay, B. B. & Strynadka, N. C. 2008 Structural analysis of the essential self-cleaving type III secretion proteins EscU and SpaS. *Nature* **453**, 124–127. (doi:10.1038/nature06832)
48 Zarivach, R., Vuckovic, M., Deng, W., Finlay, B. B. & Strynadka, N. C. 2007 Structural analysis of a prototypical ATPase from the type III secretion system. *Nat. Struct. Mol. Biol.* **14**, 131–137. (doi:10.1038/nsmb1196)
49 Lountos, G. T., Austin, B. P., Nallamsetty, S. & Waugh, D. S. 2009 Atomic resolution structure of the cytoplasmic domain of *Yersinia pestis* YscU, a regulatory switch involved in type III secretion. *Protein Sci.* **18**, 467–474. (doi:10.1002/pro.56)
50 Wiesand, U., Sorg, I., Amstutz, M., Wagner, S., van den Heuvel, J., Luhrs, T., Cornelis, G. R. & Heinz, D. W. 2009 Structure of the type III secretion recognition protein YscU from *Yersinia enterocolitica*. *J. Mol. Biol.* **385**, 854–866. (doi:10.1016/j.jmb.2008.10.034)
51 Deane, J. E., Graham, S. C., Mitchell, E. P., Flot, D., Johnson, S. & Lea, S. M. 2008 Crystal structure of Spa40, the specificity switch for the *Shigella flexneri* type III secretion system. *Mol. Microbiol.* **69**, 267–276. (doi:10.1111/j.1365-2958.2008.06293.x)
52 Fadouloglou, V. E., Tampakaki, A. P., Glykos, N. M., Bastaki, M. N., Hadden, J. M., Phillips, S. E., Panopoulos, N. J. & Kokkinidis, M. 2004 Structure of HrcQB-C, a conserved component of the bacterial type III secretion systems. *Proc. Natl Acad. Sci. USA* **101**, 70–75. (doi:10.1073/pnas.0304579101)
53 Marlovits, T. C., Kubori, T., Sukhan, A., Thomas, D. R., Galán, J. E. & Unger, V. M. 2004 Structural insights into the assembly of the type III secretion needle complex. *Science (New York, NY)* **306**, 1040–1042. (doi:10.1126/science.1102610)
54 Minamino, T., Imada, K. & Namba, K. 2008 Mechanisms of type III protein export for bacterial flagellar assembly. *Mol. Biosyst.* **4**, 1105–1115. (doi:10.1039/b808065h)
55 Thomas, D. R., Francis, N. R., Xu, C. & DeRosier, D. J. 2006 The three-dimensional structure of the flagellar rotor from a clockwise-locked mutant of

Salmonella enterica serovar Typhimurium. *J. Bacteriol.* **188**, 7039–7048. (doi:10.1128/JB.00552-06)
56 Schraidt, O., Lefebre, M. D., Brunner, M. J., Schmied, W. H., Schmidt, A., Radics, J., Mechtler, K., Galan, J. E. & Marlovits, T. C. 2010 Topology and organization of the *Salmonella typhimurium* type III secretion needle complex components. *PLoS Pathog.* **6**, e1000824. (doi:10.1371/journal.ppat.1000824)
57 Sani, M., Allaoui, A., Fusetti, F., Oostergetel, G. T., Keegstra, W. & Boekema, E. J. 2007 Structural organization of the needle complex of the type III secretion apparatus of *Shigella flexneri*. *Micron* **38**, 291–301. (doi:10.1016/j.micron.2006.04.007)
58 Mahajan, A., Yuan, C., Lee, H., Chen, E. S., Wu, P. Y. & Tsai, M. D. 2008 Structure and function of the phosphothreonine-specific FHA domain. *Sci Signal.* **1**, re12. (doi:10.1126/scisignal.151re12)
59 Korotkov, K. V., Gonen, T. & Hol, W. G. 2011 Secretins: dynamic channels for protein transport across membranes. *Trends Biochem. Sci.* **36**, 433–443. (doi:10.1016/j.tibs.2011.04.002)
60 Nouwen, N., Ranson, N., Saibil, H., Wolpensinger, B., Engel, A., Ghazi, A. & Pugsley, A. P. 1999 Secretin PulD: association with pilot PulS, structure, and ion-conducting channel formation. *Proc. Natl Acad. Sci. USA* **96**, 8173–8177. (doi:10.1073/pnas.96.14.8173)
61 Nouwen, N., Stahlberg, H., Pugsley, A. P. & Engel, A. 2000 Domain structure of secretin PulD revealed by limited proteolysis and electron microscopy. *EMBO J.* **19**, 2229–2236. (doi:10.1093/emboj/19.10.2229)
62 Kazmierczak, B. I., Mielke, D. L., Russel, M. & Model, P. 1994 pIV, a filamentous phage protein that mediates phage export across the bacterial cell envelope, forms a multimer. *J. Mol. Biol.* **238**, 187–198. (doi:10.1006/jmbi.1994.1280)
63 Linderoth, N. A., Model, P. & Russel, M. 1996 Essential role of a sodium dodecyl sulfate-resistant protein IV multimer in assembly-export of filamentous phage. *J. Bacteriol.* **178**, 1962–1970.
64 Linderoth, N. A., Simon, M. N. & Russel, M. 1997 The filamentous phage pIV multimer visualized by scanning transmission electron microscopy. *Science* **278**, 1635–1638. (doi:10.1126/science.278.5343.1635)
65 Collins, R. F., Davidsen, L., Derrick, J. P., Ford, R. C. & Tonjum, T. 2001 Analysis of the PilQ secretin from *Neisseria meningitidis* by transmission electron microscopy reveals a dodecameric quaternary structure. *J. Bacteriol.* **183**, 3825–3832. (doi:10.1128/JB.183.13.3825-3832.2001)
66 Opalka, N., Beckmann, R., Boisset, N., Simon, M. N., Russel, M. & Darst, S. A. 2003 Structure of the filamentous phage pIV multimer by cryo-electron microscopy. *J. Mol. Biol.* **325**, 461–470. (doi:10.1016/S0022-2836(02)01246-9)
67 Reichow, S. L., Korotkov, K. V., Hol, W. G. & Gonen, T. 2010 Structure of the cholera toxin secretion channel in its closed state. *Nat. Struct. Mol. Biol.* **17**, 1226–1232. (doi:10.1038/nsmb.1910)
68 Korotkov, K. V., Pardon, E., Steyaert, J. & Hol, W. G. 2009 Crystal structure of the N-terminal domain of the secretin GspD from ETEC determined with the assistance of a nanobody. *Structure* **17**, 255–265. (doi:10.1016/j.str.2008.11.011)
69 Mishima, M., Shida, T., Yabuki, K., Kato, K., Sekiguchi, J. & Kojima, C. 2005 Solution structure of the peptidoglycan binding domain of *Bacillus subtilis* cell wall lytic enzyme CwlC: characterization of the sporulation-related repeats by NMR. *Biochemistry* **44**, 10 153–10 163.
70 Valverde, R., Edwards, L. & Regan, L. 2008 Structure and function of KH domains. *FEBS J.* **275**, 2712–2726. (doi:10.1111/j.1742-4658.2008.06411.x)
71 Kimbrough, T. G. & Miller, S. I. 2000 Contribution of *Salmonella typhimurium* type III secretion components to needle complex formation. *Proc. Natl Acad. Sci. USA* **97**, 11 008–11 013. (doi:10.1073/pnas.200209497)
72 Kubori, T., Sukhan, A., Aizawa, S. I. & Galán, J. E. 2000 Molecular characterization and assembly of the needle complex of the *Salmonella typhimurium* type III protein secretion system. *Proc. Natl Acad. Sci. USA* **97**, 10 225–10 230. (doi:10.1073/pnas.170128997)
73 Tamano, K., Aizawa, S., Katayama, E., Nonaka, T., Imajoh-Ohmi, S., Kuwae, A., Nagai, S. & Sasakawa, C. 2000 Supramolecular structure of the *Shigella* type III secretion machinery: the needle part is changeable in length and essential for delivery of effectors. *EMBO J.* **19**, 3876–3887. (doi:10.1093/emboj/19.15.3876)
74 Broz, P., Mueller, C. A., Muller, S. A., Philippsen, A., Sorg, I., Engel, A. & Cornelis, G. R. 2007 Function and molecular architecture of the *Yersinia* injectisome tip complex. *Mol. Microbiol.* **65**, 1311–1320. (doi:10.1111/j.1365-2958.2007.05871.x)
75 Marlovits, T. C., Kubori, T., Lara-Tejero, M., Thomas, D., Unger, V. M. & Galán, J. E. 2006 Assembly of the inner rod determines needle length in the type III secretion injectisome. *Nature* **441**, 637–640. (doi:10.1038/nature04822)
76 Akeda, Y. & Galan, J. E. 2005 Chaperone release and unfolding of substrates in type III secretion. *Nature* **437**, 911–915. (doi:10.1038/nature03992)
77 Bishop, M. F. & Ferrone, F. A. 1984 Kinetics of nucleation-controlled polymerization. A perturbation treatment for use with a secondary pathway. *Biophys. J.* **46**, 631–644. (doi:10.1016/S0006-3495(84)84062-X)
78 Botteaux, A., Sani, M., Kayath, C. A., Boekema, E. J. & Allaoui, A. 2008 Spa32 interaction with the inner-membrane Spa40 component of the type III secretion system of *Shigella flexneri* is required for the control of the needle length by a molecular tape measure mechanism. *Mol. Microbiol.* **70**, 1515–1528. (doi:10.1111/j.1365-2958.2008.06499.x)
79 Journet, L., Agrain, C., Broz, P. & Cornelis, G. R. 2003 The needle length of bacterial injectisomes is determined by a molecular ruler. *Science* **302**, 1757–1760. (doi:10.1126/science.1091422)
80 Wood, S. E., Jin, J. & Lloyd, S. A. 2008 YscP and YscU switch the substrate specificity of the *Yersinia* type III secretion system by regulating export of the inner rod protein YscI. *J. Bacteriol.* **190**, 4252–4262. (doi:10.1128/JB.00328-08)
81 Cornelis, G. R. 2006 The type III secretion injectisome. *Nat. Rev. Microbiol.* **4**, 811–825. (doi:10.1038/nrmicro1526)
82 Zhang, L., Wang, Y., Olive, A. J., Smith, N. D., Picking, W. D., De Guzman, R. N. & Picking, W. L. 2007 Identification of the MxiH needle protein residues responsible for anchoring IpaD to the type III secretion needle tip. *J. Biol. Chem.* **282**, 32 144–32 151. (doi:10.1074/jbc.M703403200)
83 Espina, M. *et al.* 2006 IpaD localizes to the tip of the type III secretion system needle of *Shigella flexneri*. *Infect Immun.* **74**, 4391–4400. (doi:10.1128/IAI.00440-06)
84 Mueller, C. A., Broz, P., Muller, S. A., Ringler, P., Erne-Brand, F., Sorg, I., Kuhn, M., Engel, A. & Cornelis, G. R. 2005 The V-antigen of *Yersinia* forms a distinct structure at the tip of injectisome needles. *Science* **310**, 674–676. (doi:10.1126/science.1118476)
85 Sani, M., Botteaux, A., Parsot, C., Sansonetti, P., Boekema, E. J. & Allaoui, A. 2007 IpaD is localized at

the tip of the *Shigella flexneri* type III secretion apparatus. *Biochim. Biophys. Acta* **1770**, 307–311. (doi:10.1016/j.bbagen.2006.10.007)
86 Wilson, R. K., Shaw, R. K., Daniell, S., Knutton, S. & Frankel, G. 2001 Role of EscF, a putative needle complex protein, in the type III protein translocation system of enteropathogenic *Escherichia coli*. *Cell Microbiol.* **3**, 753–762. (doi:10.1046/j.1462-5822.2001.00159.x)
87 Bergman, T., Hakansson, S., Forsberg, A., Norlander, L., Macellaro, A., Backman, A., Bolin, I. & Wolf-Watz, H. 1991 Analysis of the V antigen lcrGVH-yopBD operon of *Yersinia pseudotuberculosis*: evidence for a regulatory role of LcrH and LcrV. *J. Bacteriol.* **173**, 1607–1616.
88 Lara-Tejero, M. & Galan, J. E. 2009 *Salmonella enterica* serovar Typhimurium pathogenicity island 1-encoded type III secretion system translocases mediate intimate attachment to nonphagocytic cells. *Infect. Immun.* **77**, 2635–2642. (doi:10.1128/IAI.00077-09)
89 Menard, R., Sansonetti, P. & Parsot, C. 1994 The secretion of the *Shigella flexneri* Ipa invasins is activated by epithelial cells and controlled by IpaB and IpaD. *EMBO J.* **13**, 5293–5302.
90 Pettersson, J. *et al.* 1999 The V-antigen of *Yersinia* is surface exposed before target cell contact and involved in virulence protein translocation. *Mol. Microbiol.* **32**, 961–976. (doi:10.1046/j.1365-2958.1999.01408.x)
91 Picking, W. L., Nishioka, H., Hearn, P. D., Baxter, M. A., Harrington, A. T., Blocker, A. & Picking, W. D. 2005 IpaD of *Shigella flexneri* is independently required for regulation of Ipa protein secretion and efficient insertion of IpaB and IpaC into host membranes. *Infect. Immun.* **73**, 1432–1440. (doi:10.1128/IAI.73.3.1432-1440.2005)
92 Wang, Y., Nordhues, B. A., Zhong, D. & De Guzman, R. N. 2010 NMR characterization of the interaction of the *Salmonella* type III secretion system protein SipD and bile salts. *Biochemistry* **49**, 4220–4226. (doi:10.1021/bi100335u)
93 Olive, A. J., Kenjale, R., Espina, M., Moore, D. S., Picking, W. L. & Picking, W. D. 2007 Bile salts stimulate recruitment of IpaB to the *Shigella flexneri* surface, where it colocalizes with IpaD at the tip of the type III secretion needle. *Infect. Immun.* **75**, 2626–2629. (doi:10.1128/IAI.01599-06)
94 Veenendaal, A. K., Hodgkinson, J. L., Schwarzer, L., Stabat, D., Zenk, S. F. & Blocker, A. J. 2007 The type III secretion system needle tip complex mediates host cell sensing and translocon insertion. *Mol. Microbiol.* **63**, 1719–1730. (doi:10.1111/j.1365-2958.2007.05620.x)
95 Sanowar, S. *et al.* 2010 Interactions of the transmembrane polymeric rings of the *Salmonella enterica* serovar Typhimurium type III secretion system. *MBio.* **1**, e00158-10. (doi:10.1128/mBio.00158-10)
96 Wagner, S., Konigsmaier, L., Lara-Tejero, M., Lefebre, M., Marlovits, T. C. & Galan, J. E. 2010 Organization and coordinated assembly of the type III secretion export apparatus. *Proc. Natl Acad. Sci. USA* **107**, 17 745–17 750. (doi:10.1073/pnas.1008053107)
97 Diepold, A., Amstutz, M., Abel, S., Sorg, I., Jenal, U. & Cornelis, G. R. 2010 Deciphering the assembly of the *Yersinia* type III secretion injectisome. *EMBO J.* **29**, 1928–1940. (doi:10.1038/emboj.2010.84)
98 Diepold, A., Wiesand, U. & Cornelis, G. R. 2011 The assembly of the export apparatus (YscR,S,T,U,V) of the *Yersinia* type III secretion apparatus occurs independently of other structural components and involves the formation of an YscV oligomer. *Mol. Microbiol.* **82**, 502–514. (doi:10.1111/j.1365-2958.2011.07830.x)
99 Sorg, J. A., Miller, N. C., Marketon, M. M. & Schneewind, O. 2005 Rejection of impassable substrates by *Yersinia* type III secretion machines. *J. Bacteriol.* **187**, 7090–7102. (doi:10.1128/JB.187.20.7090-7102.2005)
100 Sukhan, A., Kubori, T., Wilson, J. & Galan, J. E. 2001 Genetic analysis of assembly of the *Salmonella enterica* serovar Typhimurium type III secretion-associated needle complex. *J. Bacteriol.* **183**, 1159–1167. (doi:10.1128/JB.183.4.1159-1167.2001)
101 Mueller, C. A., Broz, P. & Cornelis, G. R. 2008 The type III secretion system tip complex and translocon. *Mol. Microbiol.* **68**, 1085–1095. (doi:10.1111/j.1365-2958.2008.06237.x)
102 Minamino, T. & Namba, K. 2008 Distinct roles of the FliI ATPase and proton motive force in bacterial flagellar protein export. *Nature* **451**, 485–488. (doi:10.1038/nature06449)
103 Galan, J. E. 2008 Energizing type III secretion machines: what is the fuel? *Nat. Struct. Mol. Biol.* **15**, 127–128. (doi:10.1038/nsmb0208-127)